Environmental Modelling & Software 26 (2011) 778–786

Contents lists available at ScienceDirect

Environmental Modelling & Software

journal homepage: www.elsevier.com/locate/envsoft

A cokriging based approach to reconstruct air pollution maps, processing measurement station concentrations and deterministic model simulations

Vikas Singh, Claudio Carnevale, Giovanna Finzi, Enrico Pisoni*, Marialuisa Volta

Department of Electronics for Automation, University of Brescia, Via Branze 38, I-25123 Brescia, Italy

ARTICLE INFO

Article history:
Received 9 November 2009
Received in revised form
15 June 2010
Accepted 29 November 2010
Available online 19 January 2011

Keywords:
Spatial interpolation
Cokriging
Air quality modeling
Ozone
PM10

ABSTRACT

One of the aims of regional Environmental Authorities is to provide citizens information about the quality of the atmosphere over a certain region. To reach this objective Environmental Authorities need suitable tools to interpolate the data coming from monitoring networks to domain locations where no measures are available. In this work a spatial interpolation system has been developed to estimate 8-h mean daily maximum ozone concentrations and daily mean PM10 concentrations over a domain, starting from measured concentration values. The presented approach is based on a cokriging technique, using the results of a deterministic Chemical Transport Model (CTM) simulation as secondary variable. The developed methodology has been tested over a 60×60 km^2 domain located in Northern Italy, including Milan metropolitan area, one of the most polluted areas in Europe.

1. Introduction

Air pollution monitoring is a major issue in Europe, because it is a possible approach to understand pollutants distribution over a domain, and consequently to develop suitable emission control policies (Carnevale et al., 2009; Pisoni et al., 2009a). Spatial interpolation techniques are an easy-to-use and effective way to estimate pollutant levels in areas where no measurements are available (Isaaks and Srivastava, 1990; Denby et al., 2005; EPA, 2004), starting from monitoring station measurements. Interpolation can also be used to spatialize point wise forecasting performed with stochastic techniques (Pisoni et al., 2009b). There are different techniques available to perform spatial interpolation, that can be classified as deterministic or stochastic. The deterministic ones include the nearest-neighbor and polynomial interpolation (Inverse distance weighted) approaches (EPA, 2004; Isaaks and Srivastava, 1990). The stochastic methods refer to geostatistical approaches such as kriging (Beelen et al., 2009; Jourdan, 2009) and cokriging (Cressie, 1993; Isaaks and Srivastava, 1990). In particular the literature presents applications of kriging to map background air pollution data as NO_2, PM10, O_3, SO_2, CO (Beelen et al., 2009). But the problem of kriging (as of other similar spatialization techniques) is related to the fact that its performances are heavily affected by the number and spatial distribution of monitoring stations available.

For this reason in the cokriging approach additional data (supposed to be correlated to the one to be spatialized) are provided through an intensive sampled secondary variable (Deutsch and Journel, 1997; Isaaks and Srivastava, 1990). Hooyberghs et al. (2006) presents the cokriging based RIO (residual interpolation) model for spatial interpolation of ambient ozone concentrations from sparse monitoring points in Belgium, using population density as auxiliary data to remove spatial trend due to titration effect. Janssen et al. (2008) extends the RIO model to PM10 and NO_2 using CORINE land cover data as an indicator for interpolation. Also Royle et al. (1999) propose a multivariate interpolation method to estimate the daily ozone, similar to cokriging and kriging with external drift.

This paper proposes a novel approach to estimate the ozone and PM10 concentrations at unmonitored locations applying a cokriging technique using, as secondary variable, the seasonal simulations of the 3D Transport Chemical Aerosol Model TCAM (Carnevale et al., 2008a, 2008b). The proposed methodology has been formalized and applied over an urban area centered in Milan, one of the most polluted areas in Europe. The paper is structured as follows: in Section 2 the proposed methodology is presented, Section 3 discusses the case study set-up, Section 4 the validation results and Section 5 the conclusions.

* Corresponding author. Tel.: +39 030 3715520; fax: +39 030 380014.
E-mail address: enrico.pisoni@ing.unibs.it (E. Pisoni).

1364-8152/$ – see front matter © 2010 Elsevier Ltd. All rights reserved.
doi:10.1016/j.envsoft.2010.11.014

2. The proposed methodology

Let Ψ be a function whose values are measured in a limited number of points $X = \{x_1, \ldots, x_P\}$ of a three-dimensional space. The proposed methodology has the objective to estimate the value of in all the points $W = \{w_1, \ldots, w_I\}$ at a regular grid over a certain domain. In general $\Psi(W)$ is computed as a function f of the measured values of $\psi(X)$ and of other information $\xi(V)$ over the same domain ($V = \{v_1, \ldots, v_S\}$).

$$\Psi(W) = f(\psi(x_1), \ldots, \psi(x_P), \xi(v_1), \ldots, \xi(v_S)) \tag{1}$$

The interpolation procedure is performed at each time t, when a set of measured values $\psi(X)$ is available.

In the next subsections the formalization of the implemented methodology is presented.

2.1. Kriging

The kriging estimates the value of the function $\Psi(W)$ as a linear combination of the values $\psi(X)$:

$$\Psi(W) = K\psi(X) \tag{2}$$

where K is the linear combination coefficient vector. Weights $K = [k_{i,p}]$ (with i representing the grid point w_i where to calculate Ψ value, and p representing the monitoring station location x_P) are computed on the basis of the knowledge of the semi-variogram, which describes the expected squared increment of the values ψ between location pairs x_p and x_q. The empirical semi-variogram γ_ψ is constructed as:

$$\gamma_\psi(\overline{d}) = \frac{1}{2N(\overline{d})} \sum_{(p,q)} \left[\psi(x_p) - \psi(x_q)\right]^2 \tag{3}$$

where $N(\overline{d})$ is the number of monitoring station pairs (x_p, x_q) separated by the distance $\overline{d}$. Then, the empirical semi-variogram is fitted by a model $\widehat{\gamma}_\psi$ which is used to solve, for each $w_{i,}$ the system of $P + 1$ equations (Isaaks and Srivastava, 1989):

$$\sum_{p=1}^{P} k_{i,p} \widehat{\gamma}_\psi(d_{x_p,x_q}) + \mu = \widehat{\gamma}_\psi(d_{w_i,x_q}) \quad q = 1, \ldots, P \tag{4}$$

$$\sum_{p=1}^{P} k_{i,p} = 1 \tag{5}$$

where:

- P is the number of monitoring stations;
- d_{x_p,x_q} and d_{w_i,x_q} are the distances between a station point (x_p) and another station point (x_q) or a grid point (w_i), respectively;
- μ is the Lagrange multiplier which ensures unbiased conditions.

2.2. Cokriging

Cokriging is an extension of kriging, allowing the use of an auxiliary variable ξ called the secondary variable, correlated to the primary one and usually more densely sampled at $V = \{v_1, \ldots, v_S\}$ ($P \ll S$). In this case, the spatialization is implemented not only as a linear combination of primary variable ψ (known in some points $\psi(X)$) but also of the secondary variables $\xi(V)$ according to the following equation:

$$\Psi(W) = K\psi(X) + L\xi(V). \tag{6}$$

The weights $K = [k_{i,p}]$ and $L = [l_{i,s}]$ are estimated on the base of the two semi-variograms γ_ψ and γ_ξ (estimated as in (3)) and the crossvariogram $\gamma_{\psi\xi}$ which describes the correlation between the two variables ψ and ξ according to:

$$\gamma_{\psi\xi}(\overline{d}) = \frac{1}{2N(\overline{d})} \sum_{(p,q)} [\psi(x_p) - \psi(x_q)(\xi(v_p) - \xi(v_q) \tag{7}$$

where $N(\overline{d})$ is the number of station pairs (x_p, x_q) separated by $\overline{d}$. Model semi-variograms ($\widehat{\gamma}_\psi$ and $\widehat{\gamma}_\xi$) and model crossvariogram ($\widehat{\gamma}_{\psi\xi}$) are then used to compute, for each $w_{i,}$ the set of weights solving the following $P + S + 2$ equations (Isaaks and Srivastava, 1989):

$$\sum_{p=1}^{P} k_{i,p} \widehat{\gamma}_\psi(d_{x_p,x_q}) + \sum_{s=1}^{S} l_{i,s} \widehat{\gamma}_{\psi\xi}(d_{v_s,x_q}) + \mu_1 = \widehat{\gamma}_\psi(d_{w_i,x_q}) \quad q = 1, \ldots, P \tag{8}$$

$$\sum_{p=1}^{P} k_{i,p} \widehat{\gamma}_{\psi\xi}(d_{x_p,v_r}) + \sum_{s=1}^{S} l_{i,s} \widehat{\gamma}_\xi(d_{v_s,v_r}) + \mu_2 = \widehat{\gamma}_{\psi\xi}(d_{w_i,v_r}) \quad r = 1, \ldots, m \tag{9}$$

$$\sum_{p=1}^{P} k_{i,p} = 1 \tag{10}$$

$$\sum_{s=1}^{S} l_{i,s} = 0 \tag{11}$$

where:

- P and S are respectively the number of data for primary and secondary variable;
- d_{x_p,x_q} and d_{x_p,v_r} are the distances between a point (x_p) of the primary variable and another point (x_q) of the primary variable or a point (v_r) of the secondary variable, respectively;
- d_{v_s,x_q} and d_{v_s,v_r} are the distances between a point (v_s) of the secondary variable and a point of the primary variable (x_q) and another point of the secondary variable (v_r), respectively;
- d_{w_i,x_q} and d_{w_i,v_r} are the distances between a grid point (w_i) and a point of the primary variable (x_q) or the secondary variable (v_r), respectively;
- μ_1 and μ_2 are the Lagrange parameters which ensure unbiased conditions.

3. The case study set-up

3.1. The study domain

Test case has been performed for the year 2004 to interpolate 8-h running average ozone daily maximum (max8h) and daily mean PM10 concentrations over a $60 \times 60\ \text{km}^2$ urban domain in Northern Italy (Fig. 1), which includes Milan metropolitan area. The domain has been divided in 144 cells of $5 \times 5\ \text{km}^2$ each.

3.2. Available measurement data

Hourly ozone and daily mean PM10 concentrations obtained from Lombardia Regional Environmental Protection Agency (ARPA) have been used as primary variable for the test case. A number of 23 ozone and 14 PM10 monitoring stations are available in the domain (Fig. 1). The filled circles represent the annual mean values at the corresponding representative stations and the station type has been indicated using different symbols.

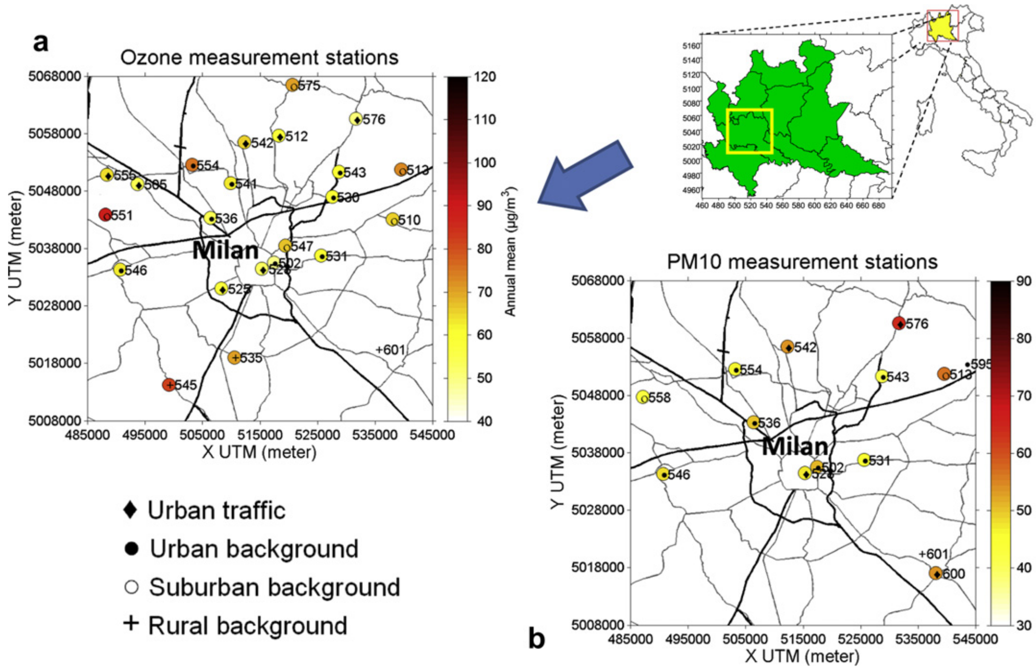

Fig. 1. Test case domain showing the measurement stations (a) Ozone (b) PM10. The filled circles represent the annual mean values of the corresponding representative stations and the symbols represent the type of the measurement stations.

3.3. *The secondary variable: TCAM simulations*

Different secondary variables can be used to implement cokriging. In this study, monthly max8h ozone and PM10 concentrations simulated in the frame of CityDelta project (Cuvelier et al., 2007) over Lombardia region with a spatial resolution of $5 \times 5\ \text{km}^2$ have been extracted and used as a secondary variable. The simulations were performed using GAMES modeling system (Volta and Finzi (2006)), consisting of three main modules: (a) the multiphase Eulerian 3D photochemical model TCAM (Transport Chemical Aerosol Model) (Carnevale et al., 2008a); (b) the meteorological preprocessor CALMET (Scire et al., 1990); (c) the emission processor POEMPM (Carnevale et al., 2006). The point sources (including stack data) and area emissions, provided by JRC, have been chemically and temporally adjusted to TCAM requirements using two inventories: one for the Lombardia Region (with $5 \times 5\ \text{km}^2$ resolution), and the EMEP one (resolution of $50 \times 50\ \text{km}^2$) (Vestreng et al., 2004) outside Lombardia Region. Meteorological fields are produced processing the outputs of ALADIN model (Berre, 2000) through CALMET. The vertical domain extends up to 3900 m a.g.l., and is subdivided into 11 layers of growing thickness. Simulations have been performed feeding the system with initial and boundary conditions by a nesting procedure from the results of the EMEP Unified Model (Simpson et al., 2003) working at a European scale. More details about the model itself and model applications can be found in Gabusi et al. (2008) and Carnevale et al. (2008a).

In the cokriging methodology presented here, these maps provide information of spatial distribution of the pollutants (ozone and PM10) to be spatialized which is driven by the emissions and meteorological conditions. As an example, monthly max8h ozone concentration for the month of July and PM10 concentration for the month of December are shown in Fig. 2(a) and (b) respectively.

3.4. *System implementation*

The system implementation has been performed using Fortran 77 GSLIB geostatistical libraries (http://www.statios.com/, http://www.gslib.com/) and Matlab® software. In particular GSLIB libraries have been used to calculate experimental semi-variogram and crossvariogram. Variogram modeling has been implemented using linear model of coregionalization, then kriging and cokriging estimates for Ozone and PM10 have been calculated. About the semi-variogram creation, for each day of simulation, two experimental semi-variograms (for ozone and PM10) are calculated for the primary and secondary data. A crossvariogram is then calculated to link primary and secondary variable. Fig. 3(a) and (b) shows the two experimental semi-variogram and the experimental cross semi-variogram with their model fits by the liner model of coregionalization, for the month of July 2004 (ozone) and December 2004 (PM10) respectively. Experimental variograms have been calculated with a lag distance of 10,000 m with lag tolerance of ± 5000 m. The calculated variograms are unidirectional in NS direction with angular tolerance of $\pm 90^\circ$. In the presence of few and widely spaced data, it is common to use a fairly large angular tolerance and lag distance to obtain enough pairs for the stable variograms (Deutsch and Journel, 1997).

3.5. *System validation procedure and performance indexes*

The system has been validated by performing leave-one-out cross validation for summer and winter in year 2004 for ozone and PM10 respectively. The value at a location is discarded from the sample dataset and the value at the same location is then estimated using the remaining sample data. This process is repeated for each location to get the estimation, which does not include the measurement data at that location.

The performance of the interpolation system was assessed by comparing the estimated values at monitoring stations $\Psi_t(X)$ and measurements $\psi_t(X)$ time series. Standard statistical indexes, such as the correlation coefficient, mean error and root mean square error were estimated.

The correlation coefficient ρ, computed for each monitoring station x_p was calculated as:

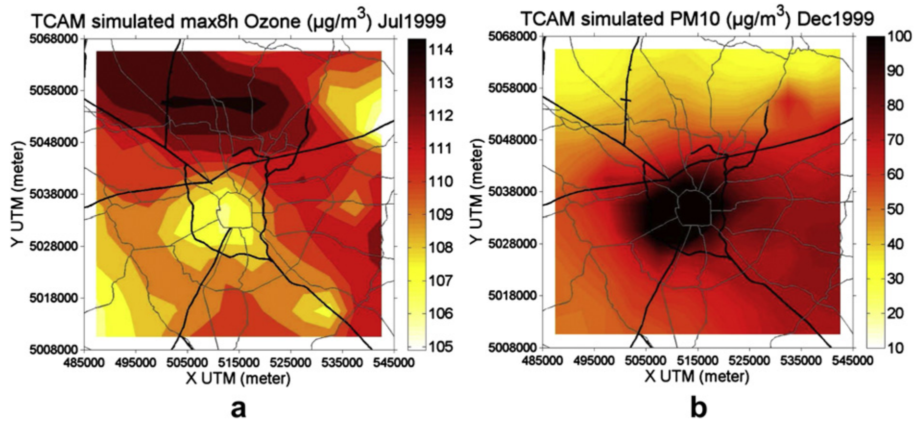

Fig. 2. Secondary variable used in cokriging (a) TCAM simulated monthly ozone concentration for August and (b) PM10 concentration for December.

$$\rho(x_p) = \frac{\frac{1}{T}\sum_{t=1}^{T}\left[\left(\Psi_t(x_p) - \mu_\Psi(x_p)\right)\cdot\left(\psi_t(x_p) - \mu_{\psi(x_p)}\right)\right]}{\sigma_\Psi \cdot \sigma_\psi} \quad (12)$$

where μ_Ψ and μ_ψ are respectively the mean of model results and of measured values; σ_Ψ and σ_ψ are their respective standard deviations and T is the number of days.

The estimation error has been defined as difference between the estimate and the measure at a fixed location (x_p). So the mean error $\varepsilon(x_p)$ and root mean square error (RMSE) have been calculated as:

$$\varepsilon(x_p) = \frac{1}{T}\sum_{t=1}^{T}\left[\Psi_t(x_p) - \psi_t(x_p)\right] \quad (13)$$

$$\mathrm{RMSE}(x_p) = \sqrt{\frac{1}{T}\sum_{t=1}^{T}\left[\Psi_t(x_p) - \psi_t(x_p)\right]^2} \quad (14)$$

In order to check the ability of the model to reproduce legislation requirements it is important to provide an accurate estimation of the values exceeding a threshold, which could have adverse effects on human health and environment.

If A represents the number of correctly estimated exceedances, F represents all estimated exceedances, M represents all observed exceedances and N is the total number of days considered, then the success of the system can be tested by using a binary system for comparison of estimated and observed occurrence of exceedances. An event is considered when the air quality level exceeds the threshold limit set by EU. It is important to correctly

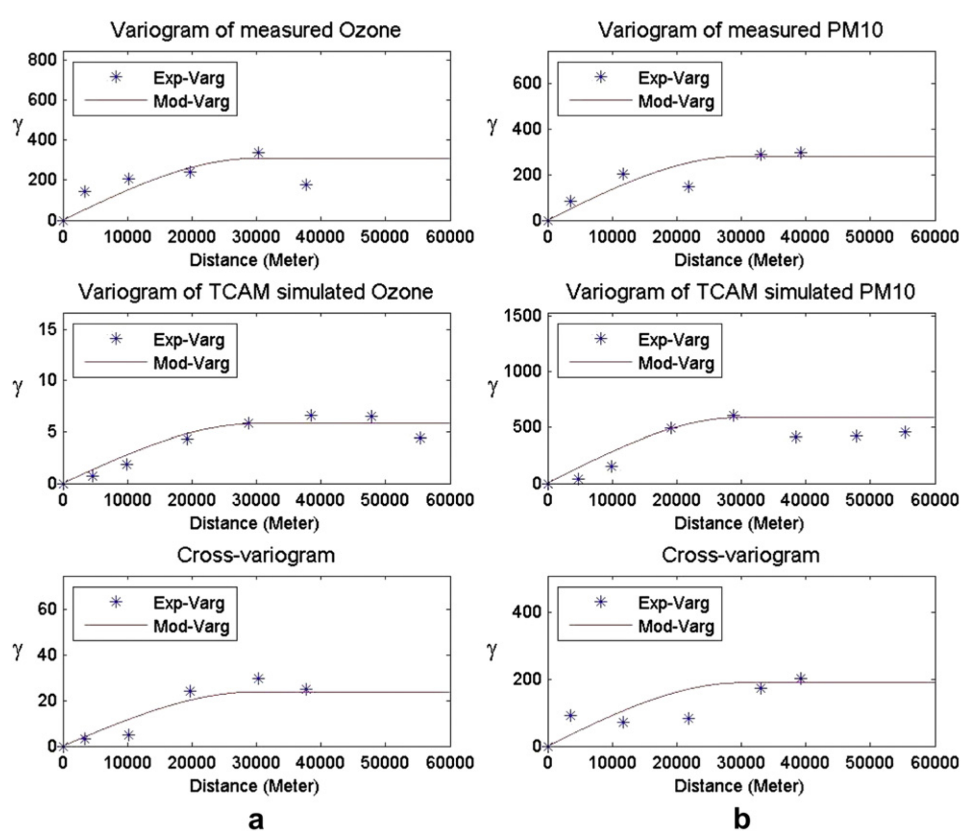

Fig. 3. Examples of experimental semi-variograms and model fits (a) for ozone in July 2004 and (b) for PM10 in December 2004.

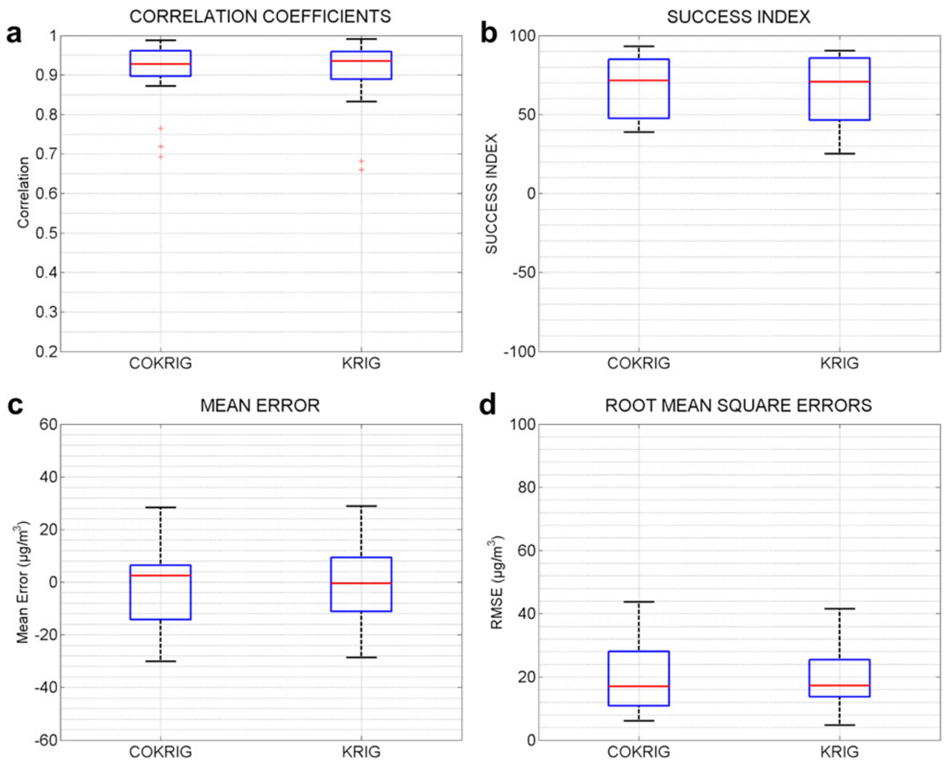

Fig. 4. Box plots of leave-one-out cross validation performance indexes for ozone in summer.

estimate, for each monitoring station (x_p), the exceedance event and non-exceedance events. The fraction of correct estimated exceedance events or probability of detection (SP) is given as SP $= (A/M)$*100%. The fraction of realized estimated exceedance events (SR) is calculated as SR $= (A/F)$*100%. Both SP and SR range from 0 to 100 with best value of 100%.

Assuming equal weights to both of the events, the scoring parameter, SP and SR can be combined to a success index (SI)

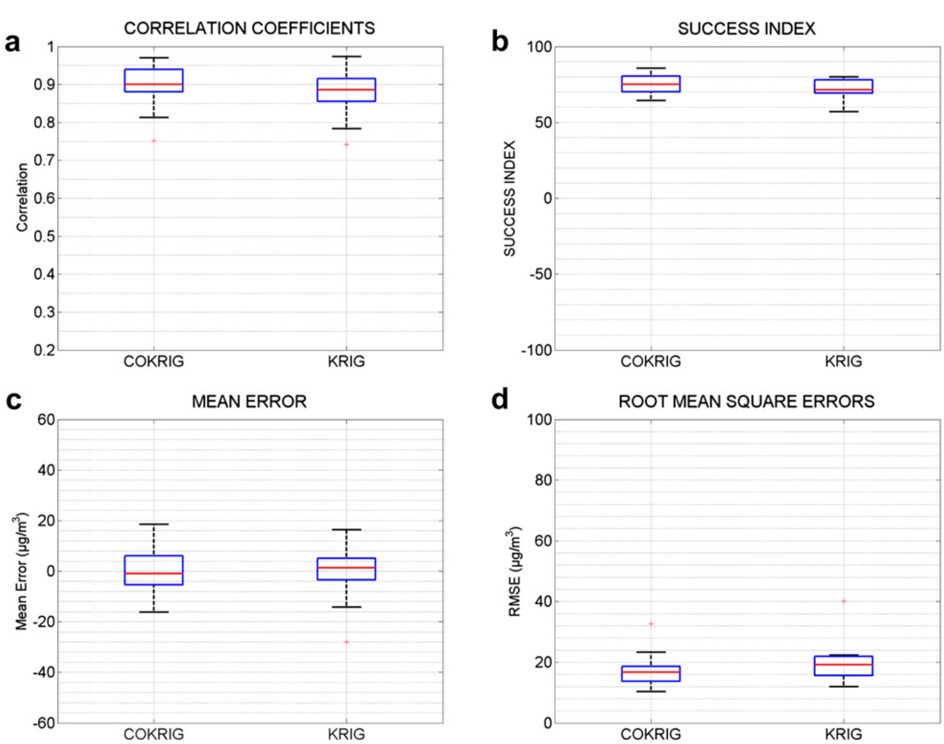

Fig. 5. Box plots of leave-one-out cross validation performance indexes for PM10 in winter.

ranging from −100 to 100 with a best value of 100 (Van Aalst and de Leeuw, 1997).

$$SI = \left(\frac{A}{M} + \frac{N + A - M - F}{N - M} - 1\right) \cdot 100 \quad (15)$$

4. Validation results and discussion

The maximum of 8-h running average (max8h) ozone concentrations and daily mean PM10 concentrations have been estimated over the domain using cokriging technique and compared with kriging interpolation. The Leave-one-out cross validation has been performed for all monitoring stations considering the entire year 2004 and seasonal performance indexes (summer for ozone and winter for PM10) have been calculated.

Figs. 4 and 5 show the box plots of the correlation coefficient, success index, mean error and root mean square error of ozone and PM10 respectively calculated for cokriging (COKRIG) and kriging (KRIG) interpolation systems obtained through cross validation. The comparison of the indexes for both techniques shows a general good agreement mainly related to higher correlations and low bias and positive success index. For ozone, having fair number of monitoring stations, no significant improvement in cokriging estimation is noticed as compared to the kriging estimation. The correlation coefficients between estimated and measured max8h ozone concentrations highlight the good agreement of the estimated time series with measured ones. The box plots in Fig. 4 (a) indicate that correlation coefficients vary between 0.90 and 0.96. The success index to estimate the critical pollution events is found to be around 70% (Fig. 4(b)). The mean error of the system is close to zero, with underestimation for some of the background urban and suburban station, moreover the RMSE of the interpolation system 18 $\mu g/m^3$ for both kriging and cokriging (Fig. 4(d)) which is around 18% of the winter mean concentration. For PM10, characterized by a smaller number of monitoring stations, slightly improvement is noticed with cokriging over kriging estimation; this is due to the use of CTM simulations as secondary variable which bring additional information at unmonitored location. The correlation coefficient for cokriging estimate (Fig. 5(a)) is found to be 0.9. The success indexes of the PM10 estimation are comparable for both kriging and cokriging (Fig. 5(b)). The mean error is found to be close to zero (Fig. 5(c)) and the RMSE shows slightly better results in the case of cokriging (Fig. 5(d)).

The scatter plots of measured values versus estimated values using cokriging for an urban background station (502) and urban traffic station (542) of ozone and PM10 are shown in Fig. 6. Each scatter plot also shows the correlation coefficient ρ, best line fit equation and the associated R^2 (correlation coefficient squared) value. These plots provide additional evidence on how the developed methodology performs. In the scatter plot, vast majority of ozone and PM10 estimates fall within ±50% of the observations with good correlation between estimated and measured values.

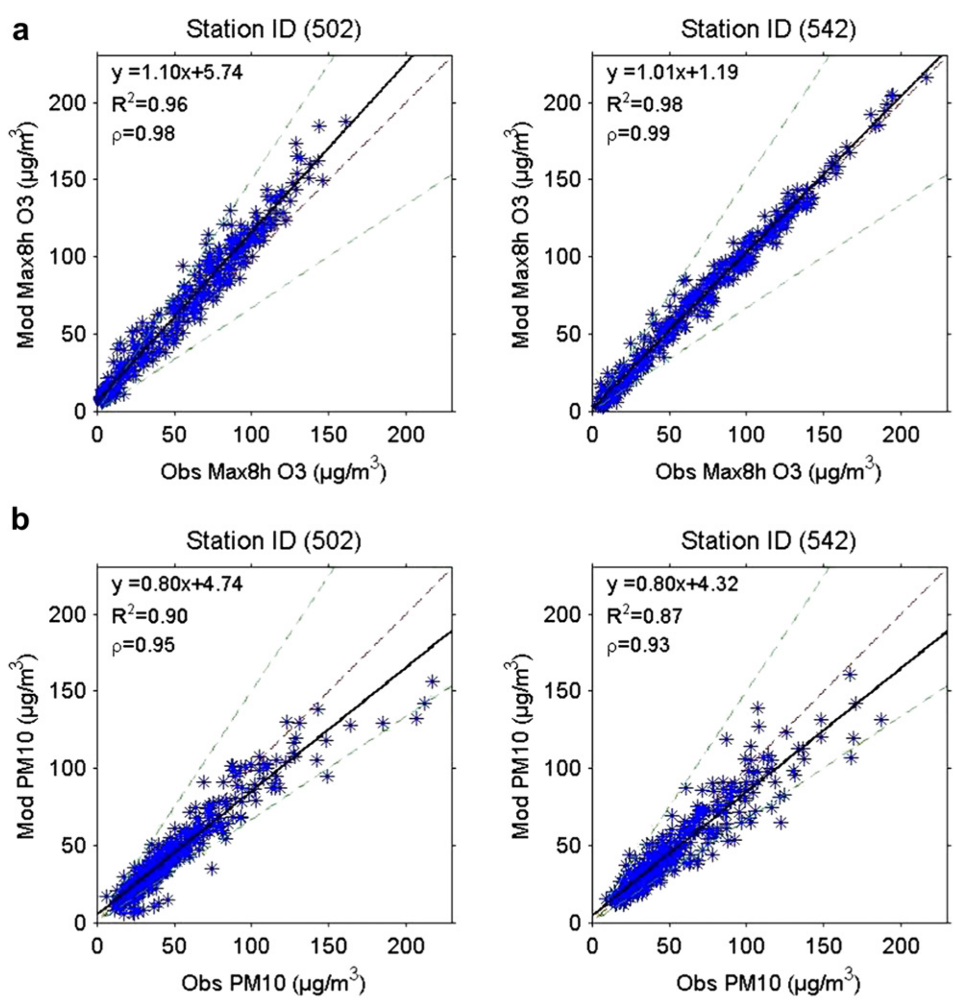

Fig. 6. Scatter plots of measured versus estimated values of (a) ozone in summer (b) PM10 in winter, at an urban background station 502 and a traffic station 542.

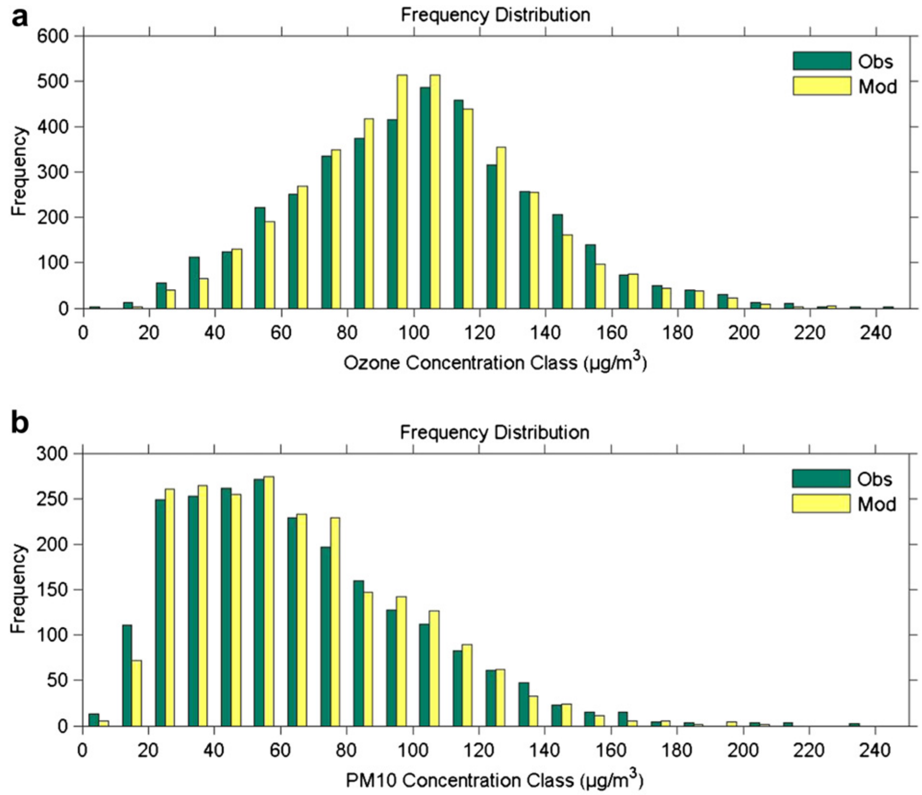

Fig. 7. Measured (OBS) and estimated (MOD) frequency distribution plotted using all stations (a) for ozone in summer and (b) for PM10 in winter.

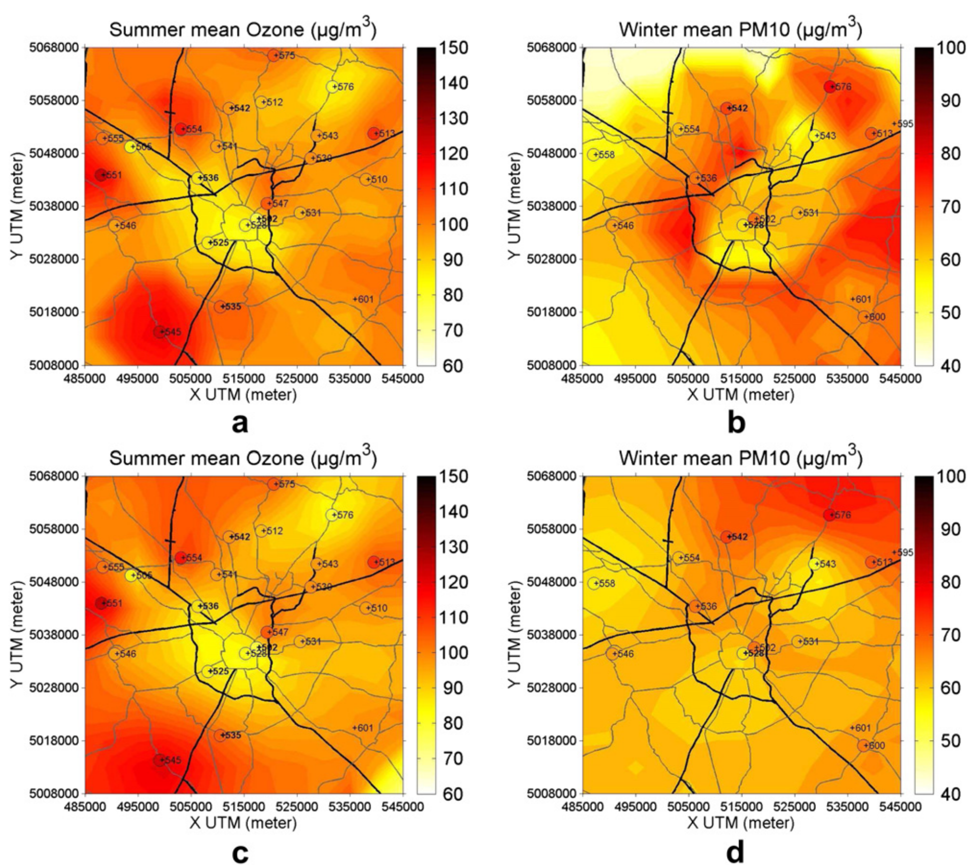

Fig. 8. Estimated concentration maps and comparison with the measurements (filled circles) (a) summer mean maximum 8 h ozone produced using cokriging; (b) winter mean PM10 produced using cokriging; (c) summer mean maximum 8 h ozone produced using kriging; (d) winter mean PM10 produced using kriging.

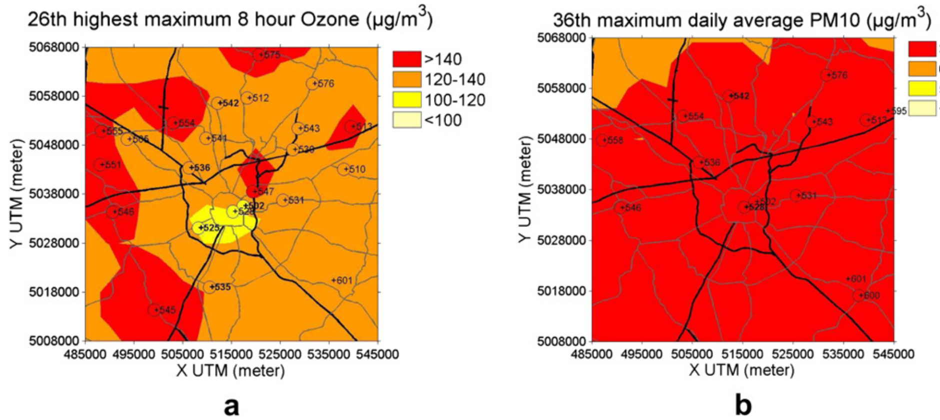

Fig. 9. Estimated exceedance concentration maps and comparison with the measurements (filled circles) (a) 26th highest maximum 8 h ozone (b) 36th highest daily mean PM10.

As for ozone (Fig. 6(a)) urban background station (502) overestimates most of the times showing positive bias and also the root mean squared error also assumes higher values as compared to station 542. This is due to the fact that concentration at station 502 is influenced by surrounded stations 528, 547 and 531 having higher values, which contributes to the large positive mean error while performing cross validation. Moreover for station 542, ozone level exceeds the threshold limit 53 days in summer, which is very well estimated by the model showing success index of 93.10%. The success index for station 502 is found to be 85.12% where only 15 days exceeds the critical limit.

As for PM10 (Fig. 6(b)), the two scatter plots are quite similar, moreover performance of the system at background urban station 502 is found slightly better than urban traffic station 542. This could be due to the fact that the traffic station is highly influenced by the local traffic emission, which is one of the important contributor in PM10 levels in the study area. The number of days exceeding the threshold limit is 111 and 129 days in winter for stations 502 and 542 respectively, which is very well estimated by the used methodology showing 80% success index.

Fig. 7(a) and (b) shows the frequency distribution of the measured (OBS) and estimated (MOD) concentrations for all station for ozone and PM10 respectively, calculated for summer and winter months using cokriging. For ozone the distribution peaks around the mean value (101.76 $\mu g/m^3$) while PM10 peaks around a wide range (20–80 $\mu g/m^3$) with mean 65.21 $\mu g/m^3$. Comparing the frequency in different classes, it is possible to appreciate the good performances of the system for almost all classes.

The estimated seasonal mean maps have been evaluated and compared qualitatively with the seasonal mean of the measurements. Fig. 8(a) and (c) shows the estimated summer mean maximum 8 h ozone concentration maps produced using cokriging and kriging techniques respectively and the filled circles represent the mean measured concentrations. As noticed in the performance indexes, ozone spatial distribution looks quite similar for both the techniques; nevertheless, looking at the location where no monitoring stations are available, cokriging ozone map shows a spatial variability more similar to the CTM one. This feature is not seen in the kriging map.

Fig. 8(b) and (d) shows the estimated winter mean PM10 concentration maps produced using cokriging and kriging techniques respectively. Here one can notice a significant difference among both maps however the comparison with the measurements looks similar. The additional information brought by CTM simulation is totally missing in kriging map, and cokriging map looks more reliable. In the absence of densely available monitoring station network, the use of CTM simulations which are governed by the emissions and meteorology can bring additional information into the construction of air pollution maps for legislation requirements.

A final comparison has been performed with respect to the air quality legislation, which sets limit values for protection of human health. As for ozone, max8h ozone concentration of 120 $\mu g/m^3$ should not be exceeded by more than 25 days per year (EC 2002/3, 2002). Fig. 9(a) shows the 26th highest maximum 8 h ozone concentration map produced using cokriging and comparison with the measurements of the representative stations. It can be noticed that the whole domain shows concentration much higher than the limiting value except for some part of the city area, which is the result of the titration effect due to the high amount of NO_x produced over city area.

As for PM10 mass concentrations (EC 1999/30, 1999), European citizens should not be exposed to daily mean levels exceeding 50 $\mu g/m^3$ for more than 35 days per year (EC 1999/30, 1999). Fig. 9 (b) shows the 36th highest daily mean PM10 concentration map produced using cokriging and comparison with the measurements of the representative stations. The whole domain shows concentrations much above critical level which is accurately estimated by the proposed method.

Both the qualitative and quantitative comparisons show the pollution maps generated using cokriging technique using CTM simulation as a secondary variable can be used for air quality and health impact assessment by the decision makers to provide information to the general public about the level of pollution where no monitoring stations are available.

5. Conclusions

In this paper, a new methodology is proposed to estimate the ozone and PM10 concentrations at unmonitored locations. To estimate the concentrations of pollutants, spatial interpolation can be performed with kriging and cokriging techniques. The cokriging allows to use a secondary data that can substantially improve the results. The primary data used for cokriging are the point measurements available within the study area, while TCAM (the CTM) simulated concentrations have been used as a secondary data. A test case has been performed over a Milan urban area by performing leave-one-out cross validation within the domain. The validation results show good performances in terms of statistical indexes. The proposed methodology provides a cost-effective, automatic and fast technique easy to be implemented over an area and is very beneficial (in comparison to kriging) over a domain not having sufficient measurement stations. Since the number of monitoring stations may vary over a period of time by inclusion and removal of a particular station, this methodology also provides the flexibility to easily include and remove stations. It also gives the capability to use satellite data as a secondary variable, a possibility that is at the moment studied as a continuation of this work.

Acknowledgments

The research has been developed in the framework of the Pilot Project QUITSAT (QUalit dell'aria mediante l'Integrazione di misure da Terra, da SAtellite e di modellistica chimica multifase e di Trasporto - contract I/035/06/0 - http://www.quitsat.it), sponsored and funded by the Italian Space Agency (ASI). Furthermore the authors acknowledge Cost Action ES0602 (Toward a European Network on Chemical Weather Forecasting and Information Systems) community.

References

Beelen, R., Hoek, G., Pebesma, E., Vienneau, D., de Hoogh, K., Briggs, D.J., 2009. Mapping of background air pollution at a fine spatial scale across the European Union. Science of the Total Environment. doi:10.1016/j.scitotenv.2008.11.048.

Berre, L., 2000. Estimation of synoptic and mesoscale forecast error covariances in a limited-area model. Monthly Weather Review 128 (3), 644–667.

Carnevale, C., Decanini, E., Volta, M., 2008a. Design and validation of a multiphase 3d model to simulate tropospheric pollution. Science of the Total Environment 390, 166–176.

Carnevale, C., Finzi, G., Pisoni, E., Volta, M., 2008b. Modelling assessment of PM10 exposure control policies in Northern Italy. Ecological Modelling 217, 219–229.

Carnevale, C., Finzi, G., Pisoni, E., Volta, M., 2009. Neuro-fuzzy and neural network systems for air quality control. Atmospheric Environment 43, 4811–4821.

Carnevale, C., Gabusi, V., Volta, M., 2006. POEM-PM: an emission model for secondary pollution control scenarios. Environmental Modelling and Software 21, 320–329.

Cressie, N., 1993. Statistics for Spatial Data, revised ed. Wiley, New York.

Cuvelier, C., Thunis, P., Vautard, R., Amann, M., Bessagnet, B., Bedogni, M., Berkowicz, R., Brandt, J., Brocheton, F., Builtjes, P., et al., 2007. CityDelta: a model intercomparison study to explore the impact of emission reductions in European cities in 2010. Atmospheric Environment 41 (1), 189–207.

Denby, B., Horálek, J., Walker, S., Eben, K., Fiala, J., 2005. Interpolation and Assimilation Methods for European Scale Air Quality Assessment and Mapping. Part I. Review and Recommendations. Tech. Rep. 2005/7. The European Topic Centre on Air and Climate Change.

Deutsch, C.V., Journel, A.G., 1997. GSLIB: Geostatistical Software Library and User's Guide. Oxford University Press, New York.

EC 1999/30, 1999. Directive 1999/30/EC of the European parliament and of the council of 22 April 1999 relating to limit value for sulphur dioxide, nitrogen dioxide and oxides of nitrogen, particulate matter and lead in ambient air.

EC 2002/3, 2002. Directive 2002/3/EC of the European parliament and of the council of 12 February 2002 relating to ozone in ambient air.

EPA, 2004. Developing Spatially Interpolated Surfaces and Estimating Uncertainty. Tech. Rep. EPA-454/R-04-004. US-EPA.

Gabusi, V., Pisoni, E., Volta, M., 2008. Factor separation in air quality simulations. Ecological Modelling 218, 383–392.

Hooyberghs, J., Mensink, C., Dumont, G., Fierens, F., 2006. Spatial interpolation of ambient ozone concentrations from sparse monitoring points in Belgium. Journal of Environmental Monitoring 8, 1129–1135.

Isaaks, E., Srivastava, R., 1990. An Introduction to Applied Geostatistics. Oxford University Press, New York.

Isaaks, E.H., Srivastava, R.M., 1989. Applied Geostatistics. Oxford University Press.

Janssen, S., Dumont, G., Fierens, F., Mensink, C., 2008. Spatial interpolation of air pollution measurements using CORINE land cover data. Atmospheric Environment 42, 4884–4903.

Jourdan, A., 2009. How to repair a second-order surface for computer experiments by kriging. Chemometrics and Intelligent Laboratory Systems 96, 108–116.

Pisoni, E., Carnevale, C., Volta, M., 2009a. Multi-criteria analysis for PM10 planning. Atmospheric Environment 43, 4833–4842.

Pisoni, E., Farina, M., Carnevale, C., Piroddi, L., 2009b. Forecasting peak air pollution levels using Narx models. Engineering Applications of Artificial Intelligence 22, 593–602.

Royle, J., Fish, U., Service, W., Berliner, M., 1999. A hierarchical approach to multivariate spatial modeling and prediction. Journal of Agricultural, Biological, and Environmental Statistics 4 (1), 29–56.

Scire, J., Insley, E., Yamartino, R., 1990. Model Formulation and User's Guide for the CALMET Meteorological Model. Tech. Rep. A025-1. California Air Resources Board, Sacramento, CA.

Simpson, D., Fagerli, H., Jonson, J., Tsyro, S., Wind, P., Tuovinen, J., 2003. Transboundary acidification, eutrophication and ground level ozone in Europe. Part I, Unified EMEP model description, EMEP status report 1 (2003), 0806–4520.

Van Aalst, R., de Leeuw, F., 1997. National ozone forecasting systems and international data exchange in Northwest Europe. Report of the Technical Working Group on Data Exchange and Forecasting for Ozone Episodes in Northwest Europe (TWG-DFO).

Vestreng, V., Adams, M., Goodwin, J., 2004. Inventory review 2004, emission data reported to CLRTAP and under the NEC directive, EMEP/EEA joint review report. Tech. rep., EMEP/MSC-W Note 1/2004. ISSN 0804-2446.

Volta, M., Finzi, G., 2006. Games, a comprehensive gas aerosol modelling evaluation system. Environmental Modelling and Software 21, 587–594. doi:10.1016/j.envsoft.2004.06.012.